Int. J. Heat Mass Transfer. Vol. 36, No. 8, pp. 2157–2163, 1993
Printed in Great Britain

0017-9310/93 $6.00+0.00

Phase change thermal storage: transient behaviour analysis of a solar receiver/storage module using the enthalpy method

C. BELLECCI
Dipartimento di Fisica, Universita' della Calabria, 87030 Rende, Italy

and

M. CONTI
Dipartimento di Matematica e Fisica, Universita' di Camerino, 62032 Camerino, Italy

(*Received* 21 *April* 1992 *and in final form* 3 *August* 1992)

Abstract—The performance of a Solar Receiver Unit with a built-in thermal storage system is simulated by the enthalpy method. It is shown that accurate results can be obtained with a simplified modelling of the forced convective heat extraction. The results indicate some criteria to determine the optimal size of the storage system.

INTRODUCTION

EFFICIENT thermal storage is a crucial point in the solar dynamic power generation. Recently a new interest developed in this field due to the space applications perspectives [1, 2]. Latent heat thermal storage in the melting and solidification of a Phase Change Material (PCM) has been proved an effective method, due to the high storage density [3]. Moreover in this case heat is charged and extracted at a fixed temperature, and the global efficiency of the conversion system can be improved.

A Solar Receiver Unit (SRU) integrated with a latent heat thermal storage facility is shown in Fig. 1. A tube is surrounded by an external coaxial cylinder; the annular gap is filled with the PCM. The SRU collects the solar radiation focused by a concentrator on the outer cylinder; a cold fluid enters into the inner tube and absorbs heat along the way.

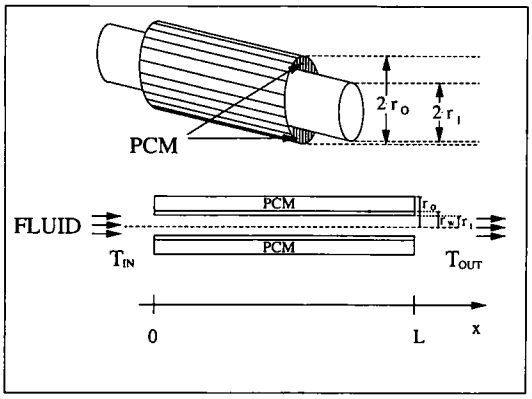

FIG. 1. Solar Receiver Unit module (SRU).

During the active phase (sunlight) the PCM melts; heat is partly supplied to the circulating fluid and is partly stored in the phase change. During the eclipse the PCM solidifies and the stored latent heat is extracted by the fluid.

A numerical description of the SRU performances requires the solution of a 'moving boundary problem' because the solid–liquid interface inside the PCM moves continuously with time, and its position is a priori unknown. Moreover, the boundary conditions on the outer wall—pulsed heat flux plus radiative losses—enhance the non-linear features of the problem.

Cao and Faghri [4] modelled a similar problem in which both the heat charge and recovery processes were performed by the circulating fluid. The outer wall of the system was assumed perfectly adiabatic. The performances of the storage module were analysed for the charge phase alone.

In their numerical study the fluid flow in the inner tube and the heat diffusion in the PCM were solved simultaneously as a conjugate problem because—they claim—significant errors could be introduced by the utilization of steady fully developed heat transfer correlations.

In this paper the transient behaviour of the SRU shown in Fig. 1 is simulated in a multiple cycle operation, until steady reproducibility is attained. The duration of the sunlight and the eclipse phases is representative for low earth orbit space applications. The enthalpy method [5–8] is utilised to treat the heat diffusion inside the SRU.

It will be shown that in normal operative conditions accurate results can be obtained if the forced con-

NOMENCLATURE

c	specific heat capacity
D	inner diameter of the SRU
F	nondimensional storage density, as defined in equation (10)
G	solar radiation intensity on the SRU outer walls
G^*	nondimensional variable, $G \cdot D/(T_M \cdot k_L)$
h	convective heat transfer coefficient
H	enthalpy per unit volume
H^*	nondimensional enthalpy, $(H-\rho_s \cdot c_s \cdot T_M)/(\rho_L \cdot \lambda)$
$\bar{H}$	enthalpy stored in the PCM, as defined in equation (11)
k	thermal conductivity
L	length of the Solar Receiver Unit (SRU)
M	PCM mass
$\dot{m}$	mass flow rate of the fluid flow
Nu	Nusselt number, $D \cdot h/k_F$
Pe	Peclet number, $Re \cdot Pr$
Pr	Prandtl number, $c_F \cdot \mu/k_F$
Q^*	nondimensional variable, $\sigma \cdot \varepsilon \cdot D \cdot T_M^3/k_L$
r_I, r_O	inner and outer radius of the SRU, respectively
r_W	radius at the wall PCM interface
Re	Reynolds number, $D \cdot \rho_F \cdot v/\mu$
S	nondimensional variable, $c_L \cdot T_M/\lambda$
t	time
t_C	duration of a full sunlight–eclipse cycle
t_{ECL}	duration of the eclipse phase in a cycle
t_{SUN}	duration of the sunlight phase in a cycle
T_O	initial temperature of the SRU
T_{IN}	fluid temperature at the inlet of the SRU
T_{OUT}	fluid temperature at the outlet of the SRU
T_M	melting temperature of the PCM
T	temperature [K]
T^*	nondimensional temperature, T/T_M
v	fluid velocity
x, r	axial and radial coordinates, respectively.

Greek symbols

α	thermal diffusivity
ε	emissivity of the SRU outer walls
θ	nondimensional variable, $G \cdot t_C/(\rho_L \cdot \lambda \cdot D)$
λ	latent heat of the PCM
μ	fluid viscosity
ξ, η	nondimensional coordinates: x/D, r/D respectively
ρ	density
σ	Stefan–Boltzman constant
χ	nondimensional variable, k_S/k_L.

Subscripts

P	PCM
S	solid phase of the PCM
L	liquid phase of the PCM
F	fluid
W	walls
MIN	minimum value
MAX	maximum value.

vection is modelled through standard experimental correlations. This allows the fluid velocity to be treated as an independent variable and to drop the continuity and momentum equations.

THE MATHEMATICAL MODEL

The heat propagation inside the SRU is governed by the energy equations, written for the fluid, the containment walls and the PCM:

Fluid

$$\frac{\partial H_F}{\partial t} + \rho_F \cdot c_F \cdot v \cdot \frac{\partial T_F}{\partial x} = \frac{4 \cdot h}{D} \cdot [T_W(r = r_I) - T_F] + k_F \cdot \frac{\partial^2 T_F}{\partial x^2} \quad (1)$$

Walls

$$\frac{\partial H_W}{\partial t} = \frac{1}{r} \cdot \frac{\partial}{\partial r}\left(k_W \cdot r \cdot \frac{\partial T_W}{\partial r}\right) + \frac{\partial}{\partial x}\left(k_W \cdot \frac{\partial T_W}{\partial x}\right) \quad (2)$$

PCM

$$\frac{\partial H_P}{\partial t} = \frac{1}{r} \cdot \frac{\partial}{\partial r}\left(k_P \cdot r \cdot \frac{\partial T_P}{\partial r}\right) + \frac{\partial}{\partial x}\left(k_P \cdot \frac{\partial T_P}{\partial x}\right). \quad (3)$$

H in equations (1)–(3) indicates the specific enthalpy, i.e. the enthalpy per unit volume, and is related to the temperature field via

$$T = A \cdot H + B \quad (4)$$

where:

Fluid

$$A = \frac{1}{\rho_F \cdot c_F}; \quad B = 0$$

Walls

$$A = \frac{1}{\rho_W \cdot c_W}; \quad B = 0$$

PCM

$$A = \frac{1}{\rho_S \cdot c_S}; \quad B = 0\,(H_P < \rho_S \cdot c_S \cdot T_M)$$

$$A = 0; \quad B = T_M \left(0 \leqslant \frac{(H_P - \rho_S \cdot c_S \cdot T_M)}{\rho_L \cdot \lambda} \leqslant 1\right)$$

$$A = \frac{1}{\rho_L \cdot c_L};$$

$$B = T_M \cdot \left(1 - \frac{\rho_S \cdot c_S}{\rho_L \cdot c_L}\right) - \frac{\lambda}{c_L}\left(\frac{H_P - \rho_S \cdot c_S \cdot T_M}{\rho_L \cdot \lambda} > 1\right).$$

We make the following assumptions:

—the heat transfer fluid is incompressible and viscous heating is neglected;
—the fluid flow is radially uniform, and the axial velocity is an independent parameter;
—heat diffusion in the containment walls is considered only at the fluid–PCM interface, i.e. zero thickness of the outer walls is assumed;
—the SRU is lighted with uniform and constant intensity during the active phase;
—heat diffusion inside the SRU is axisymmetric;
—equal duration of the sunlight and the eclipse phase: $t_{SUN} = t_{ECL} = t_C/2$;
—no natural convection inside the liquid PCM (microgravity conditions);
—convective terms due to contractions and expansions of the PCM in the phase change are neglected.

The initial and boundary conditions for equations (1–3) are specified by:

Initial conditions

$$T = T_O \quad 0 \leqslant r \leqslant r_O; \quad 0 \leqslant x \leqslant L$$

Boundary conditions

$$T = T_{IN} \quad x = 0; \quad 0 \leqslant r \leqslant r_I$$

$$\frac{\partial T}{\partial x} = 0 \quad x = 0; \quad r_I \leqslant r \leqslant r_O$$

$$\frac{\partial T}{\partial x} = 0 \quad x = L; \quad 0 \leqslant r \leqslant r_O$$

$$h \cdot (T_W - T_F) = k_W \cdot \frac{\partial T_W}{\partial r} \quad 0 \leqslant x \leqslant L; \quad r = r_I$$

$$k_W \cdot \frac{\partial T_W}{\partial r} = k_P \cdot \frac{\partial T_P}{\partial r} \quad 0 \leqslant x \leqslant L; \quad r = r_W$$

$$k_P \cdot \frac{\partial T_P}{\partial r} = G - \sigma \cdot \varepsilon \cdot T_P^4 \text{ (sunlight)}$$

$$0 \leqslant x \leqslant L; \quad r = r_O$$

$$k_P \cdot \frac{\partial T_P}{\partial r} = -\sigma \cdot \varepsilon \cdot T_P^4 \text{ (eclipse)} \quad 0 \leqslant x \leqslant L; \quad r = r_O.$$

The initial temperature T_O of the SRU is assumed uniform. The working fluid enters into the SRU at a constant temperature T_{IN}. No heat exchange is allowed through the walls normal to the SRU axis. Due to the space application only radiative losses are assumed at the outer wall.

The problem can be conveniently restated in terms of nondimensional variables. We define:

$$\eta = r/D; \quad \xi = x/D; \quad \tau = G \cdot t/(\rho_L \cdot \lambda \cdot D)$$

$$T^* = T/T_M; \quad H^* = (H - \rho_S \cdot c_S \cdot T_M)/(\rho_L \cdot \lambda)$$

$$S = c_L \cdot T_M/\lambda; \quad G^* = G \cdot D/(T_M \cdot k_L)$$

$$Q^* = \sigma \cdot \varepsilon \cdot D \cdot T_M^3/k_L; \quad \chi = k_P/k_L$$

$$\theta = G \cdot t_c/(\rho_L \cdot \lambda \cdot D).$$

In phase change problems the temperature scale is generally chosen as $(T_{IN} - T_M)$. However, our choice results in an easier treatment of the radiative losses at the outer wall. The time scale is related to the time required to melt the PCM if no heat extraction and no radiative losses occur.

The nondimensional energy equations can be written as follows:

Fluid

$$\frac{\partial H_F^*}{\partial \tau} + \frac{k_F}{k_L} \cdot \frac{Re \cdot Pr}{G^*} \cdot \frac{\partial T_F^*}{\partial \xi} = \frac{k_F}{k_L} \cdot \frac{4 \cdot Nu}{G^*} \cdot (T_W^* - T_F^*) + \frac{k_F}{k_L} \cdot \frac{1}{G^*} \cdot \frac{\partial^2 T_F^*}{\partial \xi^2} \quad (5)$$

Walls

$$\frac{\partial H_W^*}{\partial \tau} = \frac{k_W}{k_L} \cdot \frac{1}{G^*} \cdot \left(\frac{1}{\eta} \cdot \frac{\partial}{\partial \eta} \eta \cdot \frac{\partial T_W^*}{\partial \eta} + \frac{\partial^2 T_W^*}{\partial \xi^2}\right) \quad (6)$$

PCM

$$\frac{\partial H_P^*}{\partial \tau} = \frac{1}{G^*} \cdot \left(\frac{1}{\eta} \cdot \frac{\partial}{\partial \eta} \chi \cdot \eta \cdot \frac{\partial T_P^*}{\partial \eta} + \frac{\partial}{\partial \xi} \chi \cdot \frac{\partial T_P^*}{\partial \xi}\right). \quad (7)$$

The initial and boundary conditions are specified as follows:

Initial conditions

$$T^* = T_O^* \quad 0 \leqslant \eta \leqslant r_O/D; \quad 0 \leqslant \xi \leqslant L/D$$

Boundary conditions

$$T^* = T_{IN}^* \quad \xi = 0; \quad 0 \leqslant \eta \leqslant 0.5$$

$$\frac{\partial T^*}{\partial \xi} = 0 \quad \xi = 0; \quad 0.5 \leqslant \eta \leqslant r_O/D$$

$$\frac{\partial T^*}{\partial \xi} = 0 \quad \xi = L/D; \quad 0 \leqslant \eta \leqslant r_O/D$$

$$Nu \cdot \frac{k_F}{k_W} \cdot (T_W^* - T_F^*) = \frac{\partial T_W^*}{\partial \eta} \quad 0 \leqslant \xi \leqslant L/D; \quad \eta = 0.5$$

$$\frac{\partial T_W^*}{\partial \eta} = \chi \cdot \frac{k_L}{k_W} \cdot \frac{\partial T_P^*}{\partial \eta} \quad 0 \leqslant \xi \leqslant L/D; \quad \eta = r_W/D$$

$$\frac{\partial T_P^*}{\partial \eta} = \frac{G^*}{\chi} - \frac{Q^*}{\chi} \cdot T_P^{*4} \quad \text{(sunlight)}$$

$$0 \leqslant \xi \leqslant L/D; \quad \eta = r_O/D$$

$$\frac{\partial T_P^*}{\partial \eta} = -\frac{Q^*}{\chi} \cdot T_P^{*4} \quad \text{(eclipse)}$$

$$0 \leqslant \xi \leqslant L/D; \quad \eta = r_O/D.$$

The nondimensional enthalpy is related to the temperature via

$$T^* = A^* \cdot H^* + B^* \tag{8}$$

where:

Fluid

$$A^* = \frac{1}{S} \cdot \frac{\rho_L \cdot c_L}{\rho_F \cdot c_F}; \quad B^* = \frac{\rho_S \cdot c_S}{\rho_F \cdot c_F}$$

Walls

$$A^* = \frac{1}{S} \cdot \frac{\rho_L \cdot c_L}{\rho_W \cdot c_W}; \quad B^* = \frac{\rho_S \cdot c_S}{\rho_W \cdot c_W}$$

PCM

$$A^* = \frac{1}{S} \cdot \frac{\rho_L \cdot c_L}{\rho_S \cdot c_S}; \quad B^* = 1 \; (H_P^* < 0)$$

$$A^* = 0; \quad B^* = 1 \; (0 \leqslant H_P^* \leqslant 1)$$

$$A^* = \frac{1}{S}; \quad B^* = 1 - \frac{1}{S} (H_P^* > 1).$$

It can be observed that the temperature field in the SRU depends on

$$\tau, \quad S, \quad \frac{\rho_S \cdot c_S}{\rho_L \cdot c_L}, \quad \frac{\rho_W \cdot c_W}{\rho_L \cdot c_L}, \quad \frac{\rho_F \cdot c_F}{\rho_L \cdot c_L},$$

$$Pe, \quad Nu, \quad \frac{k_F}{k_L}, \quad \frac{k_W}{k_L}, \quad \chi, \quad G^*, \quad T_O^*,$$

$$\frac{r_O}{D}, \quad \frac{L}{D}, \quad \frac{r_W}{D}, \quad T_{IN}^*, \quad Q^*, \quad \theta.$$

Equations (5)–(7) have been approximated by a fully implicit difference scheme. The resulting algebraic equations were solved by the successive over-relaxations method. Due to the intrinsic non-linearity of the problem, some iterations were needed at each time step. The consistency of the computational scheme has been checked by performing an overall energy balance at each time step: energy is conserved within 0.01% of the absorbed solar radiation.

NUMERICAL RESULTS

To the authors' knowledge no experimental data are available to validate the present model. However, some significative results have been checked against the numerical solution quoted from Cao and Faghri for a hollow cylinder with adiabatic outer walls [4].

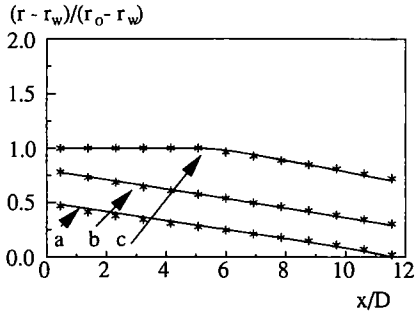

FIG. 2. Melting front positions at different times. Curve a: $vt/D = 150$; curve b: $vt/D = 400$; curve c: $vt/D = 1000$. Lines: as calculated by Cao and Faghri [4]; asterisks: present study. The set of nondimensional parameters that characterizes the solution is specified in Table 1.

The comparison is shown in Fig. 2 where the position of the melting front inside the PCM at different times is represented. The set of nondimensional parameters that characterizes the solution according to the choice of Cao and Faghri is specified in Table 1. The Nusselt number in equation (5) has been quoted from the numerical results of Chen and Chiou for liquid metals in the thermal and velocity entry length region [9].

It can be observed from the figure that the agreement is quite satisfactory. It is worth noting that the very small L/D ratio that is utilised can be considered unrealistic from a technical point of view; at higher values of L/D the entry length effects lose their importance and the present model should operate even better. The Nusselt number values were obtained for steady state conditions, while the present problem is an intrinsically transient one. However, two distinct time scales can be recognised: the flight time of the fluid inside the SRU is small if compared with the transient time of the phase change process; that is why the model does not suffer for the use of steady state Nusselt number values.

The model has been utilised to show the influence of the geometrical features on the performances of the SRU in a multiple cycle operation. The effect of the flow characteristics, i.e. of the Peclet number, is investigated too.

Lithium fluoride has been chosen as the PCM, due to the high heat of fusion and a melting temperature

Table 1.

Re	2200
Pr	0.0065
$c_L \cdot (T_{IN} - T_M)/\lambda$	0.5
$(T_O - T_M)/(T_{IN} - T_M)$	−0.1
c_S/c_L	1
k_S/k_L	1
α_L/α_F	0.02
α_W/α_F	0.11
k_F/k_W	1.42
k_L/k_W	0.124
r_O/D	1.325
r_W/D	0.575
L/D	12

Table 2.

$\rho_S \cdot c_S/(\rho_L \cdot c_L)$	1.24
$\rho_F \cdot c_F/(\rho_L \cdot c_L)$	5.53×10^{-4}
$\rho_W \cdot c_W/(\rho_L \cdot c_L)$	0.815
k_F/k_L	3.55×10^{-2}
k_W/k_L	25.6
S	2.64
χ	2.31
T_0^*	1
T_{IN}^*	0.847
r_W/D	0.575
G^*	0.206
Q^*	3.71×10^{-2}
θ	2.99

suited for power production applications. The working fluid (air) is operated at a pressure of 6×10^5 Pa. In Table 2 the values of the nondimensional parameters that have been utilised in this investigation are shown.

In these conditions the Nusselt number is determined by the well-known Colburn equation [10]:

$$Nu = 0.023 \cdot Pr^{0.3} \cdot Re^{0.8}. \quad (9)$$

Two leading criteria underlie an efficient design of the SRU:

(i) the oscillations of the fluid outlet temperature T_{OUT} in a cycle, due to the alternating sunlight and eclipse phases, should be kept in a narrow range;

(ii) economy in the storage mass and size must be pursued, especially in space-based applications.

Figure 3 shows the oscillations of T_{OUT}^* at different values of the Peclet number vs time. The curves indicate that steady reproducibility is attained after few cycles. Increasing the Peclet number results in higher fluid mass flow rates; as a consequence T_{OUT}^* lowers and all the SRU works on the average at lower temperatures. Low slope ranges can be observed, due to the quenching effect of the phase change process; high slope ranges indicate, however, that overheating

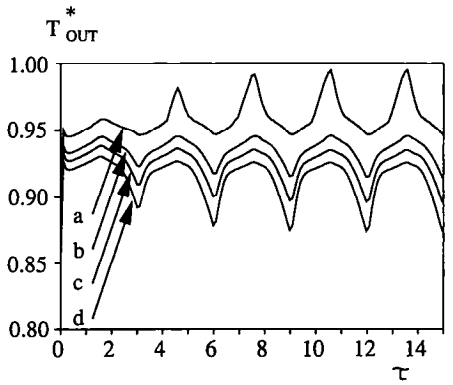

FIG. 3. Fluid temperature at the outlet of the SRU. $L/D = 120$; $r_O/D = 1.8$; curve a: $Pe = 23\,000$; curve b: $Pe = 34\,500$; curve c: $Pe = 41\,500$; curve d: $Pe = 50\,500$. The other nondimensional parameters that characterize the solution are specified in Table 2.

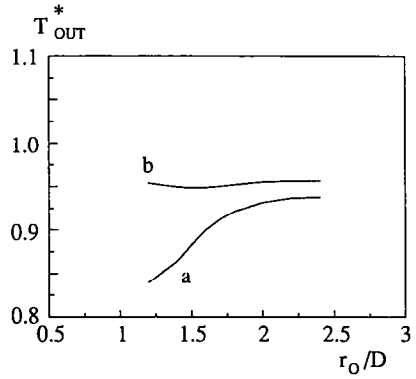

FIG. 4. Fluid temperature at the outlet of the SRU vs r_O/D; curves a, b represent the minimum and the maximum values, respectively, in a steady cycle. $L/D = 120$; $Pe = 32\,000$. The other nondimensional parameters that characterize the solution are specified in Table 2.

and/or subcooling of the PCM occurs during the cycle.

Figure 4 shows the maximum and minimum values of T_{OUT}^* in a steady cycle vs r_O/D. It should be mentioned that steady reproducibility is attained within the first five cycles even at large r_O/D, i.e. at a large thermal inertia of the SRU. We can observe that low r_O/D values cannot ensure efficient damping of the T_{OUT}^* oscillations; on the other side increasing r_0/D results in high storage mass. However, the figure shows that poor improvement in the T_{OUT}^* stability is attained for $r_O/D > 2$: this is a useful indication for a proper selection of the SRU external radius.

The effect of the Peclet number on the fluid outlet temperature is shown in Fig. 5. The curves show that the maximum stability of the outlet temperature is attained, for the specified conditions, at $Pe = 32\,000$.

Figure 6 shows the effect of different L/D. The maximum T_{OUT}^* stability is attained at $L/D = 100$. T_{OUT}^* increases with L/D due to the augmented heat transfer area; saturation effects are not yet reached in the range explored.

An efficient operation of the SRU requires a large

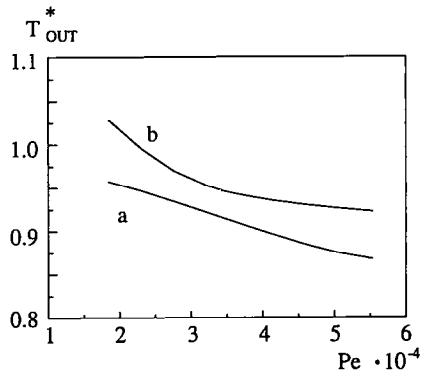

FIG. 5. Fluid temperature at the outlet of the SRU vs the Peclet number; curves a, b represent the minimum and the maximum values, respectively, in a steady cycle. $L/D = 120$; $r_O/D = 1.8$. The other nondimensional parameters that characterize the solution are specified in Table 2.

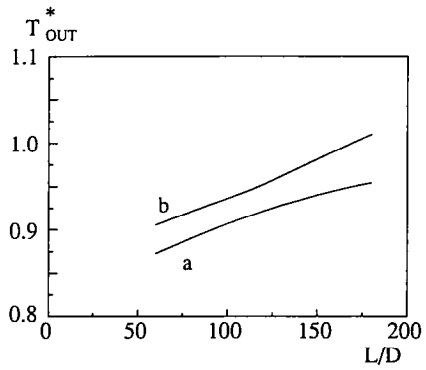

FIG. 6. Fluid temperature at the outlet of the SRU vs L/D; curves a, b represent the minimum and the maximum values, respectively, in a steady cycle. $r_O/D = 1.8$; $Pe = 32\,000$. The other nondimensional parameters that characterize the solution are specified in Table 2.

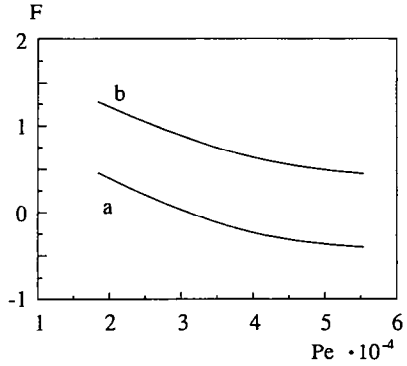

FIG. 8. F values vs the Peclet number. F is defined by equation (10). Curves a, b represent the minimum and maximum values, respectively, in a steady cycle. $r_O/D = 1.8$; $L/D = 120$. The other nondimensional parameters that characterize the solution are specified in Table 2.

heat storage density; moreover, heat should be stored as latent heat in the phase change—overheating as well as subcooling has to be avoided. The problem can be conveniently stated in terms of a nondimensional storage density, defined as

$$F = \frac{\bar{H}}{M \cdot \lambda} \tag{10}$$

where $\bar{H}$ represents the enthalpy stored in the PCM:

$$\bar{H} = \int_{V_{PCM}} (H - \rho_S \cdot c_S \cdot T_M) \cdot dx\, dy\, dz. \tag{11}$$

F represents the ratio of the enthalpy stored in the PCM to the total heat of fusion of PCM utilised.

If in a cycle $F_{MIN} < 0$ and/or $F_{MAX} > 1$ subcooling and/or overheating occurs and T^*_{OUT} runs away.

On the other side it can result $F_{MIN} > 0$ and/or $F_{MAX} < 1$; it means that only a fraction of the PCM is involved in the phase change.

In a proper design of the thermal storage F should not deviate too much from the range 0–1.

Figure 7 shows the maximum and minimum values of F in a steady cycle versus r_O/D. As expected the excursions of F decrease as r_O/D increases. The curves indicate that heavy sensible heat operation occurs at $r_O/D < 1.6$; furthermore the graph shows that for $r_O/D > 2$ a considerable amount of the PCM is excluded from the phase change. Figure 8 shows the effect of different Peclet numbers. At low Pe the SRU works 'warm' and passes to a 'cold' operation at high Pe values. A proper selection of the Peclet number should be in the range 28 000–34 000.

The effect of the SRU length is shown in Fig. 9. At low L/D subcooling inside the PCM cannot be prevented. The curves show a saturating behaviour at large L/D, where the increase of the storage mass does not compensate that of the stored heat.

CONCLUSIONS

Space based solar power generation is a matter of growing interest, and latent heat thermal storage is an effective solution to ensure stability of the thermal power delivered as well as of the operating temperatures.

A numerical model has been presented to simulate the cyclic behaviour of a Solar Receiver Unit with latent heat thermal storage. The phase change process has been treated by the enthalpy method; it has been

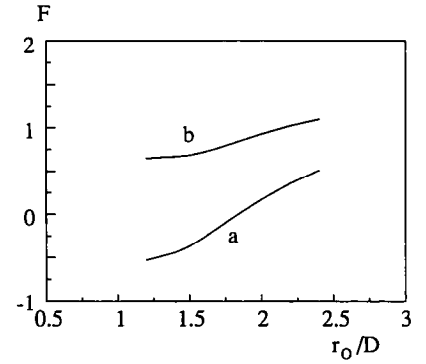

FIG. 7. F values vs r_O/D. F is defined by equation (10). Curves a, b represent the minimum and maximum values, respectively, in a steady cycle, $L/D = 120$; $Pe = 32\,000$. The other nondimensional parameters that characterize the solution are specified in Table 2.

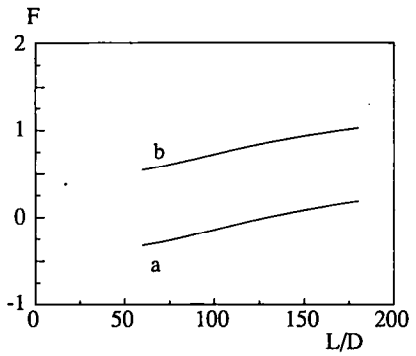

FIG. 9. F values vs L/D. F is defined by equation (10). Curves a, b represent the minimum and maximum values, respectively, in a steady cycle. $r_O/D = 1.8$; $Pe = 32\,000$. The other nondimensional parameters that characterize the solution are specified in Table 2.

shown that the convective heat extraction can be conveniently described in terms of standard heat transfer correlations. The numerical results indicate some useful criteria for a proper design of the system.

REFERENCES

1. H. J. Strumpf and M. G. Coombs, Solar receiver for the space station Brayton engine, *J. Engng Gas Turbines Power* **110,** 295–298 (1988).
2. H. J. Strumpf and M. G. Coombs, Solar receiver experiment for the space station FREEDOM Brayton engine, *J. Solar Energy Engng* **112,** 12–18 (1990).
3. R. A. Crane and G. Bharadhwaj, Evaluation of thermal energy storage devices for advanced solar dynamic systems, *J. Solar Energy Engng* **113,** 138–145 (1991).
4. Y. Cao and F. Faghri, Performance characteristics of a thermal energy storage module : a transient PCM/forced convection conjugate analysis, *Int. J. Heat Mass Transfer* **34,** 93–101 (1991).
5. R. M. Furzeland, A comparative study of numerical methods for moving boundary problems, *J. Inst. Math. Appl.* **26,** 411–429 (1980).
6. V. Voller and M. Cross, Accurate solutions of moving boundary problems using the enthalpy method, *Int. J. Heat Mass Transfer* **24,** 545–556 (1981).
7. F. Civan and C. M. Slipcevich, Efficient numerical solution for enthalpy formulation of conduction heat transfer with phase change, *Int. J. Heat Mass Transfer* **27,** 1428–1430 (1984).
8. D. B. Duncan, A simple and effective self-adaptive moving mesh for enthalpy formulations of phase change problems, *IMA Journal of Numerical Analysis* **11,** 55–78 (1991).
9. Ching-Jen Chen and Jenq Shing Chiou, Laminar and turbulent heat transfer in the pipe entrance region for liquid metals, *Int. J. Heat Mass Transfer* **24,** 1179–1189 (1981).
10. W. M. Kays and H. C. Perkins, *Handbook of Heat Transfer* (edited by W. M. Rohsenow and J. P. Hartnett). McGraw-Hill, New York (1973).